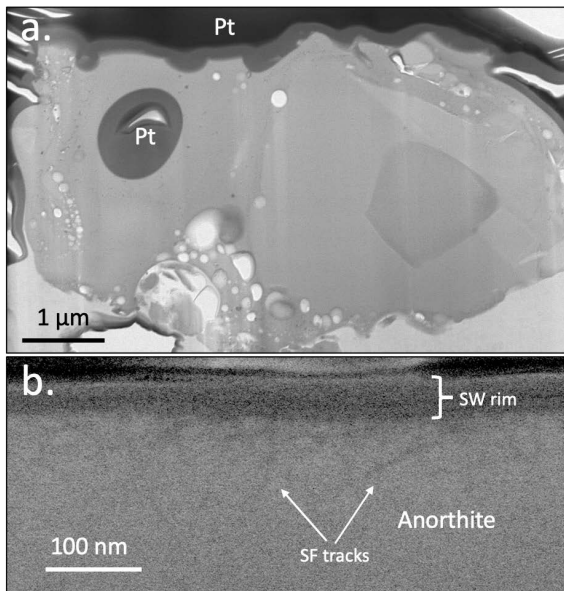


**DETECTION OF VOLATILES IN SPACE WEATHERED SURFACES.** H. A. Ishii<sup>1</sup>, J. Ciston<sup>2</sup>, J. P. Bradley<sup>1</sup>, K. K. Ohtaki<sup>1</sup>, and J. J. Gillis-Davis<sup>3</sup>, <sup>1</sup>Hawai‘i Institute for Geophysics and Planetology, University of Hawai‘i at Mānoa, Honolulu, HI 96822, USA, <sup>2</sup>National Center for Electron Microscopy, Molecular Foundry, Lawrence Berkeley National Laboratory, Berkeley, CA 94720, USA, <sup>3</sup>Washington University in St. Louis, St. Louis, MO 63130, USA (hope.ishii@hawaii.edu).

**Introduction:** The origin, abundance, chemical state, and distribution of volatiles, including water and organic compounds, are a primary focus of lunar exploration. Water is of particular significance to exploration as a resource for astronauts, future robotic missions, and fuel to explore the Solar System [1]. The presence of water ice at the lunar poles is well-established but whether its origin is primordial and a product of lunar volcanism or due to (an) ongoing, perhaps steady-state, process(es) is uncertain [2-5]. Volatile-rich micrometeorite impacts that produce lunar agglutinates are a likely volatile source [6]. Bradley et al [7] established that solar wind produces water by *in-situ* radiolysis of minerals. They discovered radiolytic water in solar wind amorphized rims on the surfaces of interplanetary dust particles (IDPs), confirmed by laboratory H<sup>+</sup> (and He<sup>+</sup>) irradiation of crystalline silicates. We focus on detection of volatiles in space weathered lunar, asteroidal and cometary surfaces. Here we discuss analyses and constraints on volatile detection in lunar regolith fines.



**Figure 1.** a) Brightfield image of a lunar agglutinate grain. b) Darkfield (HAADF) image of a lunar anorthite crystal with solar wind-generated amorphous rim and implanted solar flare tracks (density  $\sim 10^{11} \text{ cm}^{-2}$ ).

**Experimental:** We examine lunar agglutinates and solar wind irradiated amorphous rims in fines from mature lunar mare soil sample, 10084, using analytical

electron microscopy. Electron transparent sections are produced using a Helios dual beam FIB. Low-loss electron energy-loss spectroscopy (EELS) is performed using Gatan Tridium and Continuum spectrometers. Low-loss EELS can detect water (as -OH and/or H<sub>2</sub>O) and helium (via the He-K edge) with single nanometer-scale spatial resolution. Core-loss EELS is used to map iron distribution, and energy-dispersive x-ray spectroscopy using a TitanX STEM is used to map carbon distribution.

**Results:** A typical lunar agglutinate grain is shown in Figure 1a. It consists of a mixture of crystalline silicates and silicate glass. Near the surface of the agglutinate, the glass is textured and vesiculated with inclusions of nanophase-Fe (Fig. 2, inset). Low-loss EEL spectra from regions with small, still-sealed vesicles (Fig. 2) reveal no evidence of features consistent with trapped volatiles (c.f. Fig. 3). Similarly, low-loss spectra from the space weathered amorphous rim on an anorthite crystal (Fig. 1b) are also devoid of detectable volatiles.

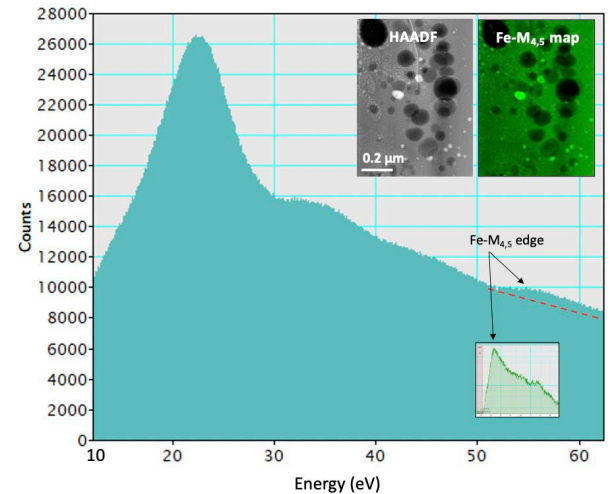


**Figure 2.** Low-loss EEL spectrum of a vesiculated region in the lower left of the agglutinate grain (Fig. 1a). No fine-structure below  $\sim 22$  eV indicates a lack of detectable -OH/H<sub>2</sub>O. Insets (upper right) are the corresponding HAADF image and Fe map (green, from the Fe-M<sub>4,5</sub> core scattering edge at  $\sim 55$  eV).

Figure 4 shows a lunar glass spherule. Like the agglutinate and rim on anorthite (Fig. 1), no low-loss features indicative of -OH/H<sub>2</sub>O were detected. However, carbon-rich inclusions associated with vesicles and other defects were observed (Fig. 4c,d).

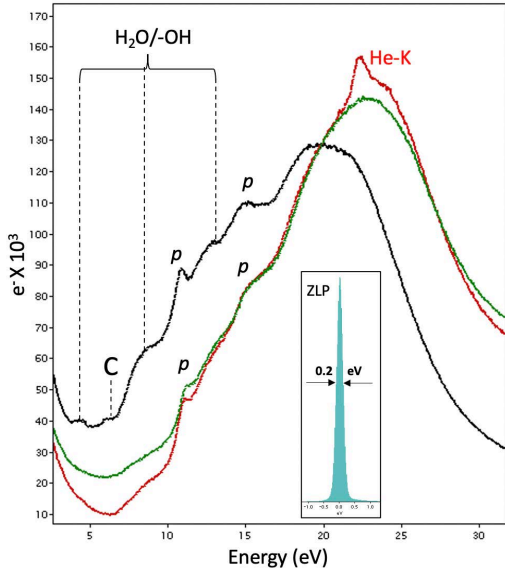


**Figure 3.** 300 keV MonoEEL spectra of experimentally irradiated rims on San Carlos olivine.  $H^+$ -irradiated (black) and  $He^+$ -irradiated on (red) and off (green) a vesicle. Features consistent with  $H_2O/-OH$ , organic carbon (C), and surface plasmons ( $p$ ) are indicated. (Inset) Energy resolution is 0.2 eV FWHM (ZLP).

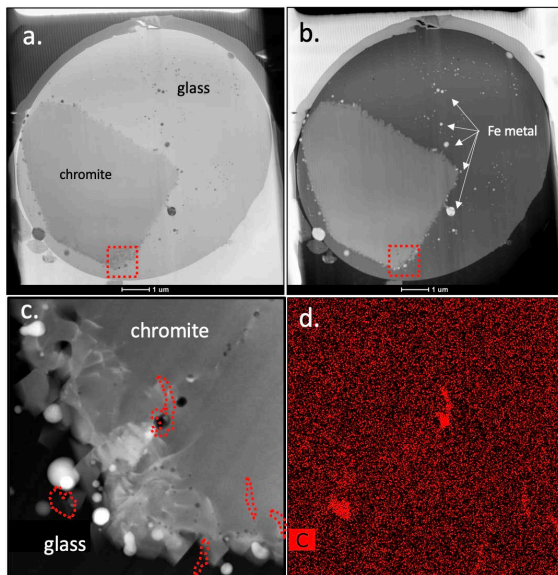


**Figure 4.** Electron transparent FIB section of a lunar glass spherule with chromite and metallic Fe inclusions. (a) STEM brightfield and (b) darkfield (HAADF) images. Red-outlined region is shown in (c) HAADF image and (d) corresponding C distribution.

**Discussion:** Although low-loss EELS is uniquely capable of detection of water and helium (and other noble gases) with high spatial resolution (Fig. 3), interpretation of spectra is non-trivial. The low-loss region is dominated by the broad volume plasmon, between 10 and 30 eV and peaked at 20-23 eV (Figs. 2

& 3). Since it is highly sensitive to solid-state variations in a sample, its intensity, shape and position can vary significantly by pixel. Superimposed on the volume plasmon in the 10-20 eV energy range are surface plasmons ( $p$ ) (Fig. 3). Because their intensities increase with nano-porosity, amorphous silicates formed by irradiation damage exhibit prominent surface plasmons (Figs. 1b & 3). In contrast, silicate glasses formed from melts lack nano-porosity (Fig. 1a), and surface plasmons are absent (Fig. 2). The volume plasmon from the  $H^+$ -irradiated surface is also broader and downward-shifted by  $\sim 3$  eV relative to the  $He^+$ -irradiated surface (Fig. 3), indicating that, in this set of irradiations, the  $H^+$ -irradiation generated more structural damage. Unambiguous detection of the He core scattering edge at  $\sim 22$  eV can be especially challenging because it is typically a weak feature and its position is close to the peak intensity of the underlying volume plasmon peak and, depending on gas pressure, can vary by 4 eV. Proper fitting of the underlying volume plasmon is important for reliable He identification.

Although radiolytic water is detected in the surfaces of some IDP grains [7], we have yet to detect water in any lunar grains by EELS. However, IDPs and lunar regolith have different thermal and sampling histories. IDPs in space are pulse heated for several seconds during atmospheric entry, although those that retain radiolytic water are unlikely to have been strongly heated. Both hydroxyl (-OH) and  $H_2O$  are detected in IDPs, the latter in vesicles that may be original (pre-atmospheric entry) or formed as a result of atmospheric entry heating [7]. Lunar equatorial soils, by contrast, are diurnally heated above 100° C and may not retain radiolytic -OH/ $H_2O$  at levels detectable by EELS [8,9]. Finally, since (organic) carbon and -OH/ $H_2O$  are common terrestrial contaminants, care must be taken during curation and specimen preparation. IDPs and this lunar soil sample were exposed to ambient air. We plan future comparison to specially curated Apollo regolith and Hayabusa asteroid regolith materials.

**Acknowledgments:** Funding by NASA grants 80NSSC19K0936 and 80NSSC20M0027 to HAI. Molecular Foundry is supported by Office of Science, BES, U.S. DOE, Contract No. DE-AC02-05CH11231.

**References:** [1] NASEM Report, (2020) Planetary Protection for the Study of Lunar Volatiles. [2] Honniball C et al. (2020) *Nat Astron*, 10.1038/s41550-02001222-x. [3] Siegler M et al. (2015) *Icarus*, 255, 78-87. [4] Syal MB (2015) *Nat Geosci* 8, 352-356. [5] Needham DH, Kring DA, (2017) *EPSL* 478, 175-178. [6] Liu Y (2012) *Nat Geosci* 5, 779-783. [7] Bradley JP et al. (2014) *PNAS* 111, 1732-1735. [8] Williams J-P et. al. (2017) *Icarus*, 283, 300-325. [9] Hayne P et. al. (2017) *JGR: Planets*, 122, 2371-2400.